# Formation of crystalline $Si_{1-x}Ge_x$ top layers by ion implantation in crystalline silicon

**A. Nélis[1], M. Chicoine[2,*], F. Schiettekatte[2], G. Terwagne[1]**

[1] LARN, Namur Institute of Structured Matter (NISM), University of Namur, B-5000 Namur, Belgium

[2]Département de Physique, Université de Montréal, Montréal, Québec, Canada

*Corresponding author email: martin.chicoine@umontreal.ca

**Abstract**. Semiconductor nanocrystals incorporated in a dielectric film are widely studied as potential candidates to exceed the Shockley-Queisser theoretical conversion limit of photovoltaic cells. In this context, Ge nanocrystals embedded in SiO2 films seem to be among the best candidates. However, the charges generated in the dielectric film are hard to collect. For this reason, it would be better if the charges were generated in a semiconductor matrix such as silicon, which has better conductivity. Implanted Ge atoms have poor mobility in a silicon-rich matrix and thus Ge nanocrystals formation is not likely. However, even if the formation of Ge nanocrystals seems difficult, it would still be interesting to form crystalline $Si_{1-x}Ge_x$ alloys. This work investigates the formation of such $Si_{1-x}Ge_x$ films by ion implantation. Those alloys could be used to improve the solar cells efficiency as the germanium concentration $x$ can be used to tune the energy gap. Fully relaxed $Si_{1-x}Ge_x$ top layers are also commonly implemented as "virtual substrates" for the growth of strained silicon layers for electronic devices. In this work, 36 keV Ge ions were implanted in crystalline Si substrates, with fluences ranging from $5 \times 10^{15}$ to $1.5 \times 10^{17}$ Ge/cm² at temperatures up to 600 °C. Rutherford Backscattering Spectrometry (RBS), Raman Spectroscopy, and Transmission Electron Microscopy (TEM) were used to investigate the microstructure of the $Si_{1-x}Ge_x$ alloys. It is shown that germanium is mostly incorporated in the crystal network in substitutional sites. XRD, Raman spectroscopy, and TEM confirm that the $Si_{1-x}Ge_x$ layer on top of the c-Si substrate is monocrystalline. TEM also indicates the possible presence of nanostructures, extended defects or both. Implantation was also carried out at temperatures up to 600 °C, with the objective of preserving the crystallinity and promoting Ge diffusion into nanoclusters. RBS shows that the Ge profile is more extended in depth for the sample implanted at 600 °C, compared to a room temperature implantation. As the energy of the ions is the same in both samples, this indicates that Ge is able to diffuse in depth during the implantation at 600°C compared to implantation at ambient temperature. However, RBS/C shows that the minimal yield is higher for the implantation at 600 °C, indicating a high concentration of interstitials or that crystallinity is deteriorated, as confirmed by TEM.

## 1. Introduction

Silicon and germanium nanocrystals incorporated in a dielectric film offer new possibilities for optoelectronic devices such as photovoltaic (PV) cells, where it could be used to exceed the Shockley-Queisser theoretical conversion limit [1-4]. Ge in particular is interesting because of its low energy bandgap, large absorption in the visible range, and its compatibility with the silicon-based manufacturing. However, the collection of the charges photogenerated inside the nanocrystals is not likely through the dielectric matrix. For this reason, it would be better if the charges were generated in a semiconductor matrix such as silicon, which has better conductivity.

Previous works [1,5,6] showed that implanted Ge atoms have a poor mobility in a silicon-rich matrix, due to the formation of strong Ge-Si chemical bonds. It was shown that, for Ge ions implanted in silicon dioxide substrates, a small excess of silicon can completely prevent the diffusion of Ge atoms, and therefore the formation of nanocrystals. It was also shown that the diffusion of Ge is enhanced in presence of a small excess of oxygen. In this context, Ge ions implanted in a Si substrate are not likely to diffuse and form nanocrystals. Moreover, the high miscibility of Ge in Si also makes the formation of Ge nanocrystals difficult. However, even if the formation of Ge nanocrystals seems difficult in Si, it would still be interesting to form crystalline $Si_{1-x}Ge_x$ alloys. Those alloys could improve the solar cells efficiency as the germanium concentration can be used to tune the energy gap between that of pure Si and that of pure Ge. Fully relaxed $Si_{1-x}Ge_x$ top layers are also commonly implemented as "virtual substrates" for the growth of strained silicon layers for electronic devices. This kind of virtual substrate is generally formed thanks to vacuum deposition techniques, using a graded concentration of Ge, whose Ge content increases from depth to surface. This gradient allows one to obtain a fully relaxed $Si_{1-x}Ge_x$ surface, while limiting the formation of defects due to lattice parameter mismatch such as dislocation. In this work, we investigate the formation of $Si_{1-x}Ge_x$ top layers as a function of Ge concentration (controlled by implantation fluence), implantation temperature, annealing temperature, and annealing time.

## 2. Experimental details

In this work, 36 keV Ge ions were implanted in crystalline Si substrates, with fluences ranging from $5 \times 10^{15}$ to $3 \times 10^{17}$ Ge/cm² at temperatures up to 600 °C. At this energy, Ge atoms are mainly implanted in the top 35 nm of the Si substrate. The angle between the beam and the

sample surface normal was set at 7° to minimize channelling. Annealing at temperatures up to 800 °C was carried out under $N_2$ atmosphere. Rutherford Backscattering Spectrometry (RBS) and channeling (RBS/C) measurements were carried out with 1 MeV He+ ions, with a backscattering angle of 170°. The channelling direction was found with a precision better than 0.1° by interpolating between planar channelling directions. The incident beam was defined by a 2-mm-diameter aperture. Samples were also characterized with Raman spectroscopy with a 514 nm laser and ×100 objective lens, Transmission Electron Microscopy (TEM) and X-ray diffraction (XRD).

## 3. **Results and discussion**

### 3.1 Implantation at room temperature

For the low projected range of Ge ions at 36 keV, the Ge concentration is expected to saturate at high fluences, at which as many Ge ions are added as there are sputtered. This is confirmed by RBS analyses (Fig. 1) which shows a saturation for fluences higher than $8 \times 10^{16}$ Ge/cm$^2$. The maximum concentration reached is about 30-31 at.% for $1.5 \times 10^{17}$ Ge/cm$^2$, as measured by RBS. TRIM simulations, treated to take sputtering and swelling effects into account, (shown as circles in Fig. 1 (a)) are in good agreement with the measured values. Retained doses are simulated using a sputtering yield of 2.34 atoms/ion extracted from the TRIM simulations. The small deviation between the measured and simulated values could be explained by the change in sputtering yield during implantation, the near-surface region of the sample being no longer composed of pure Si. RBS measurements performed before and after annealing at 800 °C (30 minutes under $N_2$ atmosphere) did not highlight any Ge diffusion or desorption, which confirms the poor mobility of Ge atoms implanted in Si.

RBS/C measurements were carried out along the <100> and <110> crystallographic orientations. Fig. 1 (b) shows the $\chi_{min}$ value, which is the ratio of the channelled and random integrated peaks along <100>. It is seen that Ge atoms are mostly incorporated in substitutional sites of the crystal network after annealing. This result was expected, as germanium has a high miscibility in silicon. However, the crystallinity of the $Si_{1-x}Ge_x$ layers deteriorates with increasing Ge fluence, which is highlighted by the increase of $\chi_{min}$. This is also illustrated in Fig. 2, which shows the RBS/C spectra for samples implanted at $4 \times 10^{16}$ and $1.5 \times 10^{17}$ Ge/cm$^2$. The inserts show the evolution of the normalized integrated Ge RBS signal in the layer compared to the Si signal in the substrate as a function of incident beam angle around the <100> orientation. Those curves show a minimum which is very close for Ge and Si for the sample implanted at $3 \times 10^{16}$ Ge/cm$^2$, indicating very good incorporation of the Ge atoms in the crystalline matrix, compared to the sample implanted at $1.5 \times 10^{17}$ Ge/cm$^2$.

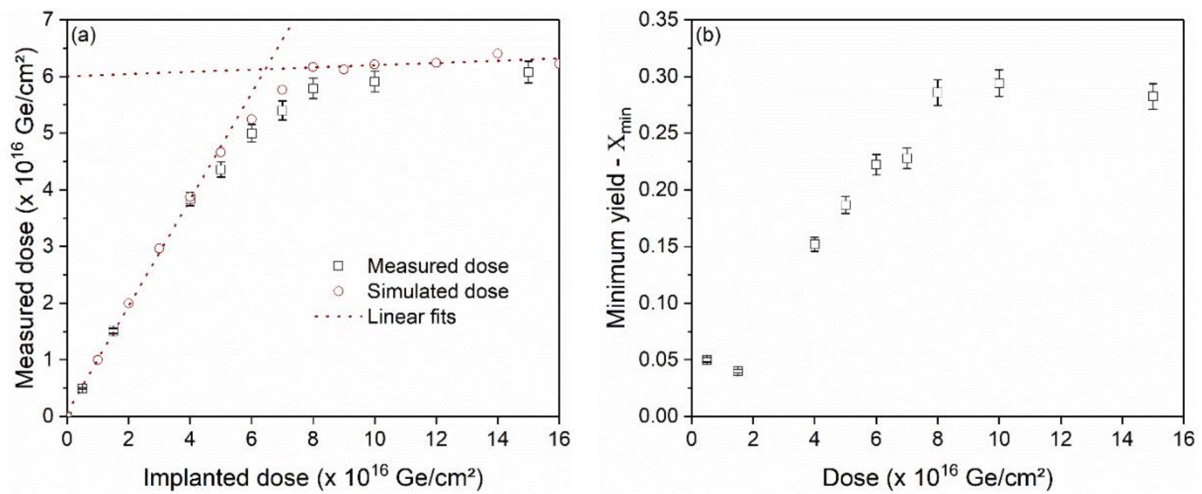


*Figure 1.* (a) Measured dose (RBS) versus implanted dose, compared to TRIM simulations taking into account sputtering and swelling effects. (b) Ratio of Ge peak integrals measured by RBS in channelled (<100>) and random orientations.

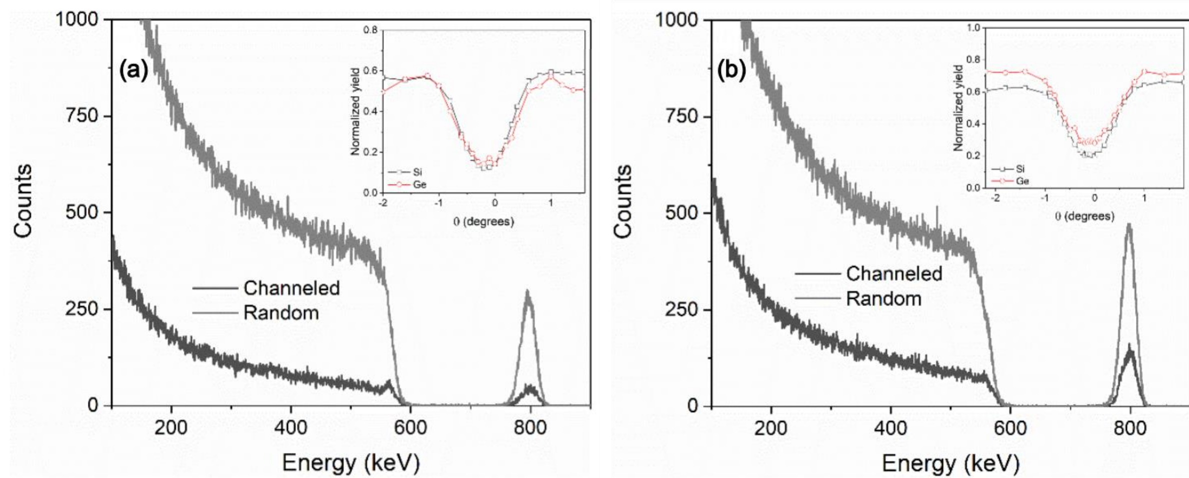


*Figure 2.* RBS/C in <100> orientation of annealed samples (800°C - 30 minutes) implanted with (a) $4 \times 10^{16}$ Ge/cm², and (b) $1.5 \times 10^{17}$ Ge/cm² at 36 keV. The insert represents angular scans for ROI in the Si substrate (behind the $Si_{1-x}Ge_x$ layer) and in the Ge peak (i.e. inside the $Si_{1-x}Ge_x$ film).

The chemical bonds of the samples was studied by Raman spectroscopy (figure 3). The Raman spectrum of c-Si has three characteristic peaks at ~302.6 cm$^{-1}$, ~434 cm$^{-1}$, and 520.7 cm$^{-1}$, which correspond to the LA, LO, and TO vibration modes respectively (yellow solid line). Three additional peaks appear after Ge implantation and annealing at 800 °C for 30 minutes under $N_2$ atmosphere. These peaks are located around 286 cm$^{-1}$, 405 cm$^{-1}$, and in the 500–520 cm$^{-1}$ range, corresponding to the Ge-Ge*, Ge-Si, and Si-Si* Raman signatures. Si-Si* is generally associated to a strained silicon layer, Si nanocrystals, or crystalline silicon containing Ge impurities. The Ge-Ge* signature has been associated to small Ge nanocrystals containing

Si impurities in Ge-implanted $SiO_2$ [1,5-8]. In the case of a Si matrix, the Ge-Ge* phonons must rather be associated to Ge-Ge bonds contaminated with Si atoms clusters that seem too small to be considered as nanocrystals. It can be seen in Figure 3 (a) that a $Si_{1-x}Ge_x$ alloy is already formed at low Ge fluence ($3 \times 10^{16}$ Ge/cm$^2$ in this case) while the Ge-Ge* signal only becomes visible at $5 \times 10^{16}$ Ge/cm$^2$. This can be explained by the weak mobility of Ge in the Si matrix, as the Ge density has to be high enough so that Ge atoms can form bonds.

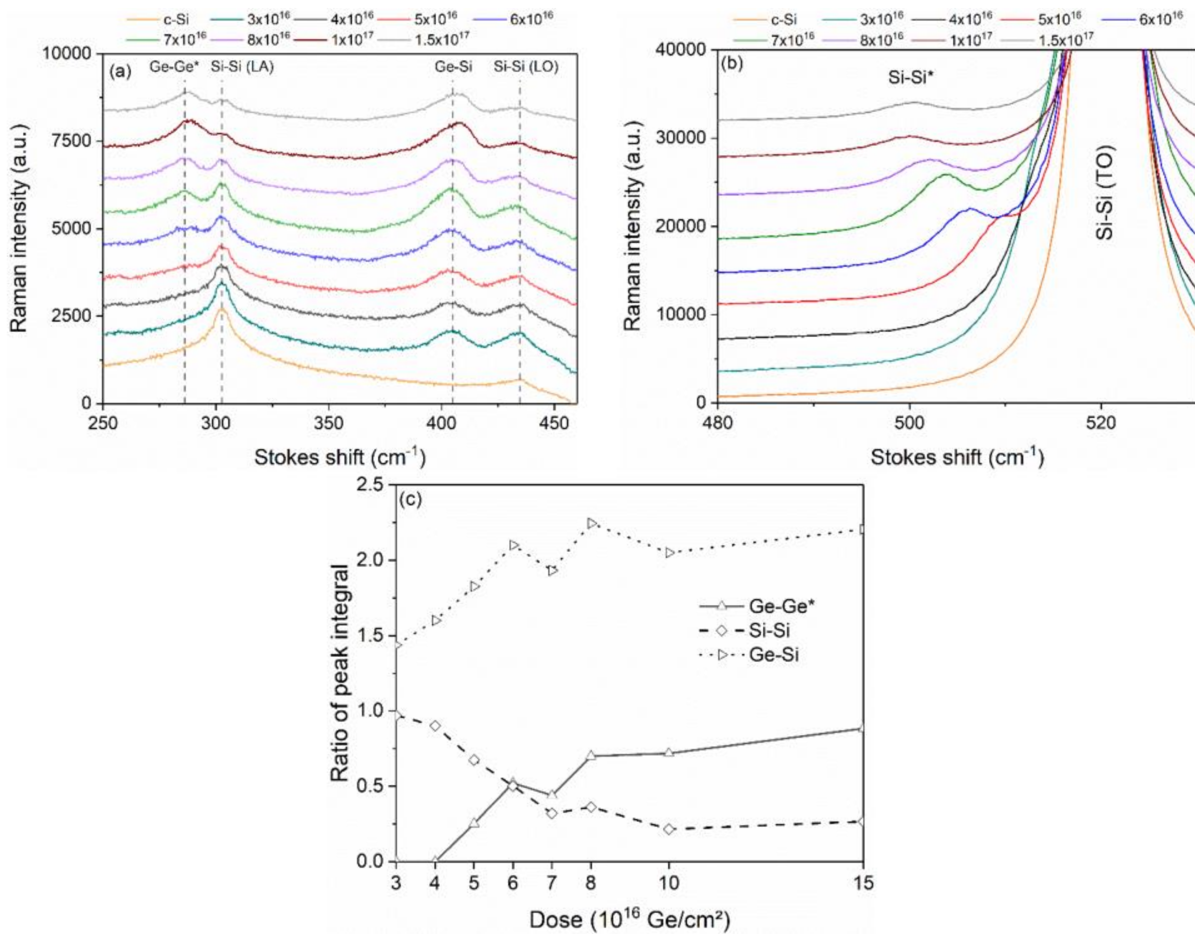


*Figure 3.* Raman spectra of samples annealed 30 minutes at 800°C for fluences varying from 3 to $1.5 \times 10^{17}$ Ge/cm$^2$ in the range (a) 250–460 cm$^{-1}$ and (b) 480–540 cm$^{-1}$. (c) Integrals of Ge-Ge*, Ge-Si and Si-Si (LA) Raman signals. The peaks integrals are divided by the integral of the signal at ~434 cm$^{-1}$ from the substrate (Si-Si LO) in order to enable a comparison between measurements.

In addition to the composition of the alloy, the shift of the Raman peaks also depends on the presence of strain in the $Si_{1-x}Ge_x$ layer. Therefore, the Ge concentration and layer strain must be determined to estimate if the peak shift is due to changes in film composition or to strain effects. RBS and XRD can be used to independently estimate the average concentration inside the $Si_{1-x}Ge_x$ layers. Lattice parameter, which depends on the alloy composition, is deduced from

peak positions in XRD measurements. Figure 4 (a) shows XRD measurements around the Si (400) peak, near 69.25°. It is seen that a peak corresponding to $Si_{1-x}Ge_x$ appears between 68° and 68.5°. The peak position, from which the interplanar distance and lattice parameter can be deduced, is shown as a function of Ge fluence in Figure 4 (b). It follows the same trend as the Ge concentration measured by RBS.

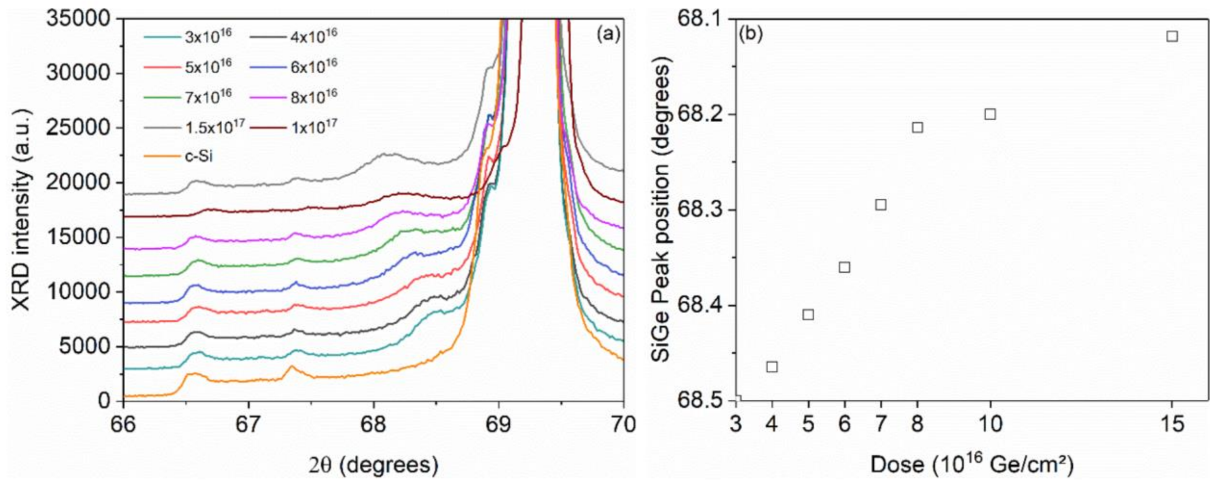


*Figure 4.* (a) XRD spectra of samples implanted with fluences ranging from $3 \times 10^{16}$ to $1.5 \times 10^{17}$ Ge/cm², annealed 30 minutes at 800 °C. (b) Evolution of SiGe (400) peak position as a function of Ge fluence.

Table 1 compares the Ge concentrations in the $Si_{1-x}Ge_x$ layers obtained by XRD and by RBS. The values are in relatively good agreement, which is an indication of the absence of high strain in the direction normal to the surface, as the peaks would be shifted by strain in the XRD spectra. Strain has been evaluated by RBS/C. Shown in Table 1 are the shifts Δθ between Si and $Si_{1-x}Ge_x$ in the <100> and <110> directions. From these values we can calculate the tetragonal strain $\varepsilon_T$ and lattice parameters ratio $a_{||}/a_{\perp}$. The weak negative values of $\varepsilon_T$ and the smaller but close to 1 values of $a_{||}/a_{\perp}$ is indicative of a very small tensile strain in the perpendicular direction. Moreover, the increase of $\chi_{min}$ with Ge fluence indicates that the films relax during thermal treatment, possibly by the formation of extended defects such as dislocations. This is in agreement with the RBS/C results showing that the crystallinity does not entirely recover after annealing, as $\chi_{min}$ varies between 0.15 and 0.30 over the range of Ge fluences, while a perfect Si crystal has a <100> $\chi_{min}$ value smaller than 0.05 for 1 MeV alpha particles.

| Ge fluence ($10^{16}/cm^2$) | XRD (at.%) | RBS (at.%) | $\Delta\theta_{<100>}$ (degrees) | $\Delta\theta_{<110>}$ (degrees) | $\varepsilon_T$ (%) | $a_{\parallel}/a_{\perp}$ | |
|---|---|---|---|---|---|---|---|
| | | | | | | Film | Substrate |
| **3** | 19.3±0.5 | - | - | - | - | - | - |
| **4** | 20.3±0.8 | 18.5±0.6 | 0.02 | 0.08 | -0.205 | 0.963 | 0.966 |
| **5** | 22.1±0.8 | 21.1±0.6 | 0.005 | 0.06 | -0.131 | 0.961 | 0.964 |
| **6** | 23.5±1.2 | 23.9±0.7 | 0.006 | 0.04 | -0.088 | 0.964 | 0.965 |
| **7** | 25.6±0.7 | 26.0±0.8 | 0.04 | - | - | - | - |
| **8** | 28.1±0.6 | 28.3±0.8 | 0.007 | 0.05 | -0.107 | 0.96 | 0.962 |
| **10** | 28.6±0.7 | 28.6±0.9 | 0.006 | 0.08 | -0.172 | 0.995 | 0.998 |
| **15** | 31.1±0.4 | 30.1±0.9 | 0.01 | 0.07 | -0.106 | 1.022 | 1.024 |

*Table 1.* Germanium concentration estimated by XRD and RBS, shifts between the Si and $Si_{1-x}Ge_x$ dips ($\Delta\theta$), tetragonal strain ($\varepsilon_T$), and lattice parameters ratios ($a_{\parallel}/a_{\perp}$).

Figure 5 shows TEM images of a Si substrate implanted with $1 \times 10^{17}$ Ge/cm$^2$ and annealed 30 minutes at 800 °C under a $N_2$ atmosphere. This image confirms the presence of a crystalline $Si_{1-x}Ge_x$ layer on top of the c-Si substrate. Images (b)-(d), taken in bright- and dark-field conditions show the possible presence of nanostructures, extended defects, or both. In particular, Figure 5 (c) highlights the presence of a large density of defects at the film/substrate interface and throughout the film, which could be associated to misfit and threading dislocations.

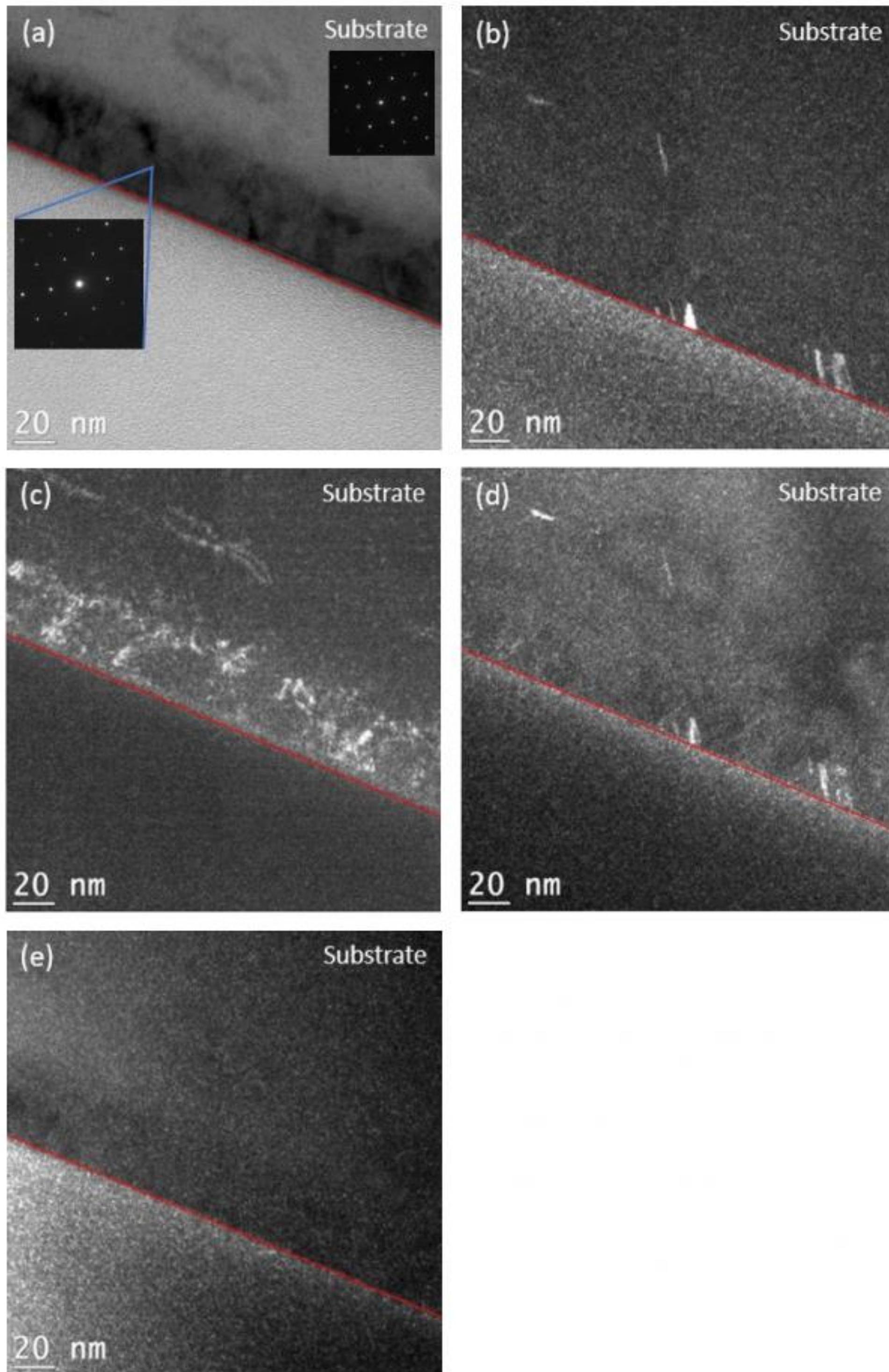


*Figure 5*. TEM micrographs of Si implanted with 1 ×$10^{17}$ Ge/$cm^2$ at 36 keV and annealed 30 minutes at 800 °C under $N_2$ atmosphere, in (a) bright filed and (b)-(e) dark filed modes. The sample surface is highlighted by a red line. The insert in (a) shows selected area diffraction patterns taken in the c-Si substrate and in the $Si_{1-x}Ge_x$ layer. The well-separated spots are indicative of a single crystalline structure.

## 3.2 Influence of annealing temperature

For annealing temperatures under 500 °C, only amorphous SiGe is observed, as observed by RBS/C or Raman spectroscopy. Figure 6 shows RBS/C spectra along <100> as a function of annealing temperature. It is seen that $\chi_{min}$ decreases with annealing temperature in both <100> and <110> crystallographic orientations, which indicates an increase of crystallinity. It is accompanied with an increase of the strain in the $Si_{1-x}Ge_x$ layer, although it remains relatively low. The decrease of $\chi_{min}$ combined with the increase of strain could indicate better incorporation of Ge in the SiGe matrix and/or lower density of defects. The results for concentration and strain as a function of annealing temperatures for samples implanted at 8 × $10^{16}$ and 1.5 × $10^{17}$ Ge /cm$^2$ at 36 keV are summarized in table 2.

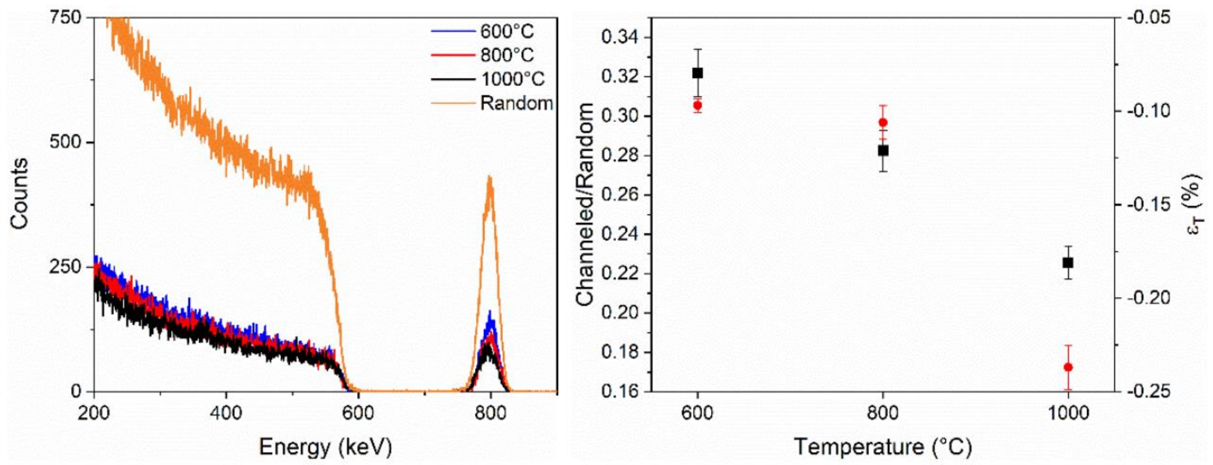


*Figure 6.* (a) RBS/C spectra of Si samples implanted with 1.5 × $10^{17}$ Ge/cm$^2$ at 36 keV and annealed at various temperatures for the random and channelled in the <100> orientations. (b) Channelled/random ratio ($\chi_{min}$, black squares) and tetragonal strain ($\varepsilon_T$, red dots) as a function of annealing temperature.

| Temperature (°C) | Fluence (Ge/cm$^2$) | $C_{Ge}$ - RBS (at.%) | $C_{Ge}$ - XRD (at.%) | $\varepsilon_T$ (%) |
|---|---|---|---|---|
| 600 | 8 × $10^{16}$ | 28.6 ± 0.9 | 27.2 ± 1.2 | -0.093 |
| 800 | | 27.7 ± 0.8 | 28.1 ± 0.6 | -0.107 |
| 1000 | | 29.4 ± 0.9 | 28.4 ± 0.3 | -0.114 |
| 600 | 1.5 × $10^{17}$ | 29.7 ± 0.9 | 30.4 ± 0.5 | -0.097 |
| 800 | | 30.5 ± 0.9 | 31.1 ± 0.4 | -0.106 |
| 1000 | | 28.9 ± 0.9 | 27.2 ± 0.5 | -0.237 |

*Table 2.* Ge concentration measured by RBS and XRD, and tetragonal strain measured by RBS/C as a function of fluence and annealing temperature after 30 minutes annealing under $N_2$ atmosphere.

Raman spectroscopy on those samples shows a decrease of the integral of the Ge-Ge* peak with increased annealing temperature for annealing temperature above 800 °C, as shown in Figure 7. This is consistent with improved crystallinity and incorporation of Ge in the crystalline matrix for annealing temperature above 800 °C.

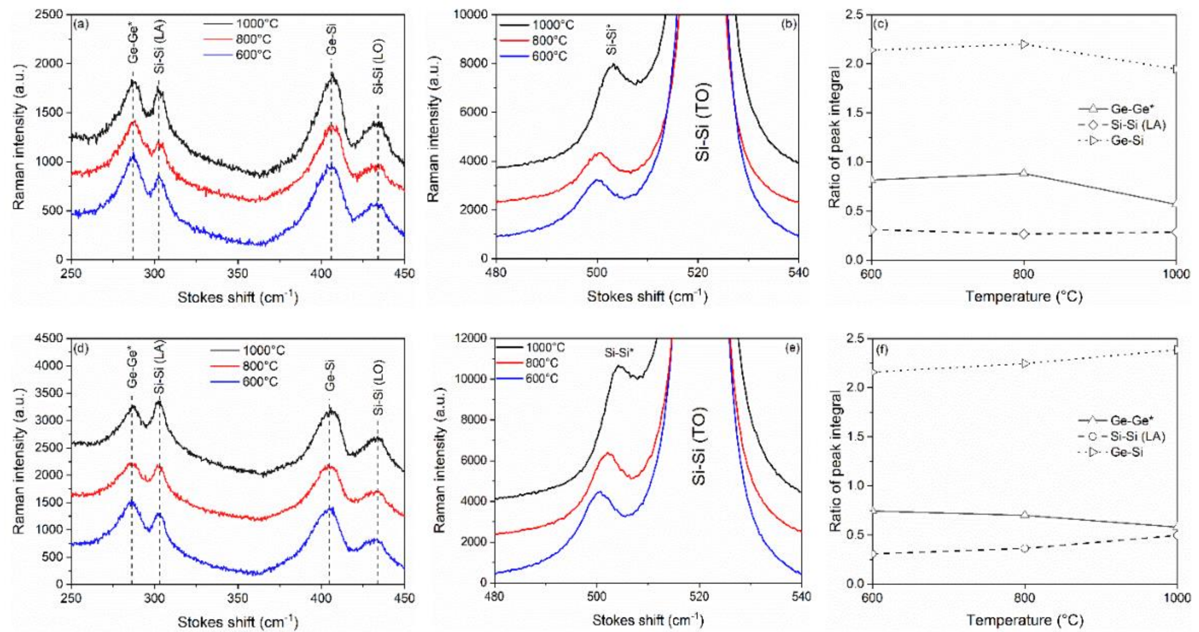


*Figure 7.* Raman spectra and integrals of the Raman peaks divided by Si-Si LO peaks for samples annealed at 800 °C with (a)-(c) $1.5 \times 10^{17}$ Ge/cm$^2$ and (d)-(f) $8 \times 10^{16}$ Ge/cm$^2$.

### 3.3 Implantation at high temperature

For the samples implanted at room temperature shown previously, the Ge concentrations measured by XRD and RBS are in close agreement. This suggests that, due to the excellent miscibility of Ge in Si, almost all Ge atoms are in substitutional sites in the $Si_{1-x}Ge_x$ alloy. This seems to prevent the formation of Ge nanocrystals. One way to make the formation of nanocrystals could be to carry out the Ge implantation at high temperature, attempting to limit Ge incorporation in Si to favour the formation of Ge nanocrystals. Two phenomena could take place. First, high-temperature implantation will prevent the amorphization of the Si matrix, which favours the formation of the alloy during the post-implantation annealing. Second, heating preserves the Si network, reducing the density of dangling bonds and thus preventing the formation of the strong Ge-Si chemical bonds. Implantation was carried out at 600 °C (temperature measured at the sample surface), a temperature high enough to instantly favour the recrystallization of Si.

Figure 8 (a) shows the RBS spectra of samples implanted at room temperature (blue lines) and at 600 °C (red lines), in random and channelled along <100> directions. Some samples were annealed 30 minutes at 800 °C under $N_2$ atmosphere. The random spectra show that the Ge profile is more extended in depth for the implantation at 600 °C. This indicates that Ge is able to diffuse during the implantation at 600 °C, compared to the room temperature implantation. This Ge diffusion possibly occurs by interstitial jumps in the preserved Si matrix. This diffusion has the effect of offsetting the Ge saturation due to sputtering that is observed with room-temperature implantations, as the measured implanted fluence ($1.01 \pm 0.03 \times 10^{17}$ Ge/cm$^2$) is the same as the nominal implanted fluence ($1 \times 10^{17}$ Ge/cm$^2$). The channelled spectra also show degraded crystallinity, and/or high concentration of interstitials, in the sample implanted at 600 °C.

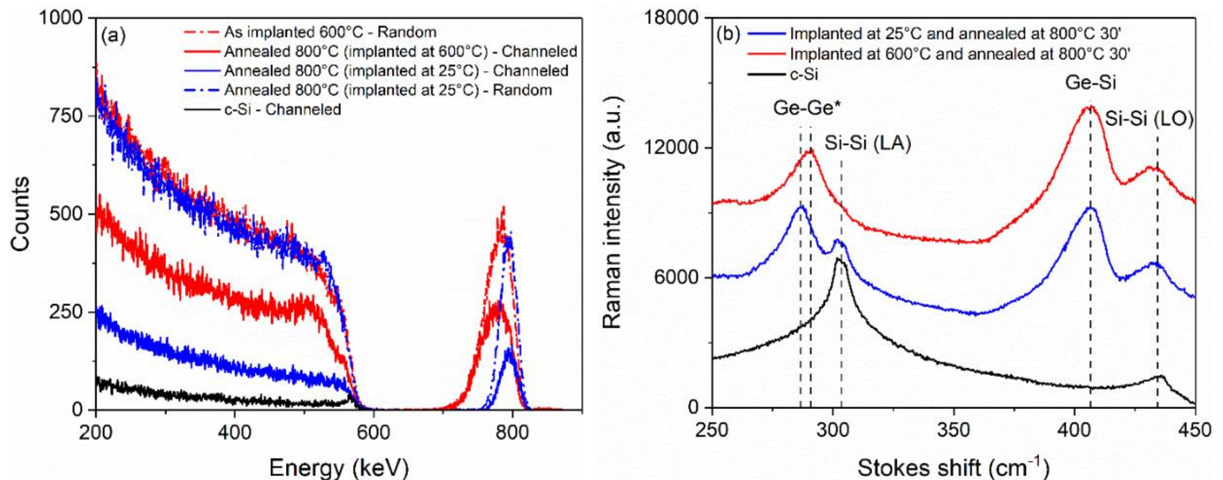


*Figure 8.* RBS/C and Raman spectra of samples implanted with $1 \times 10^{17}$ Ge/cm$^2$ at room temperature and at 600 °C and later annealed 30 minutes at 800 °C.

The Raman spectra shown in Figure 8 (b) show that the Ge-Ge* signal for the sample implanted at 600 °C is blueshifted by 4.2 cm$^{-1}$, compared to the sample implanted at room temperature. However, RBS and XRD give a lower average Ge concentration in the $Si_{1-x}Ge_x$ film. Therefore, this shift cannot be associated to an increase of the Ge concentration, which is confirmed by the position of the Si-Ge peak (~405 cm$^{-1}$), that remains the same from one sample to another. This could indicate a less efficient incorporation of the Ge atoms in the silicon matrix, favouring the formation of Ge-Ge bonds.

Figure 9 shows TEM micrographs of the sample implanted at 600 °C. TEM micrographs of the corresponding sample implanted at room temperature were already shown in Figure 5. For comparison, the images shown Figure 9 (a), (b), and (c) correspond to the images of Figure 5 (b), (e), and (a) respectively. The higher defect density seen by RBS/C for samples implanted at 600 °C (Figure 8 (a)) is also seen in Figure 8, where we see a band of dislocations at a depth between 80 and 160 nm. These dislocations extend up to the end of the implanted Ge depth profile, shown for comparison in Figure 9 (a). Figure 9 (b) reveals the presence of brighter dots, which could be associated to small nanostructures with a higher Z than Si. The depth of those nanostructures mainly corresponds to the depth of the dislocations layer. This could indicate that the Ge mobility is enhanced by the presence of structural defects, such as dislocations, and leading to the accumulation of Ge in the region containing those defects. From the analysis of the images, we estimate an average nanostructure diameter of about 1-2 nm. Note that we cannot exclude that at least a part of the nanostructures observed in Figure 9 could be formed by Ga atoms implanted during the TEM sample preparation, which was done by FIB (Focused Ion Beam) using Ga ions.

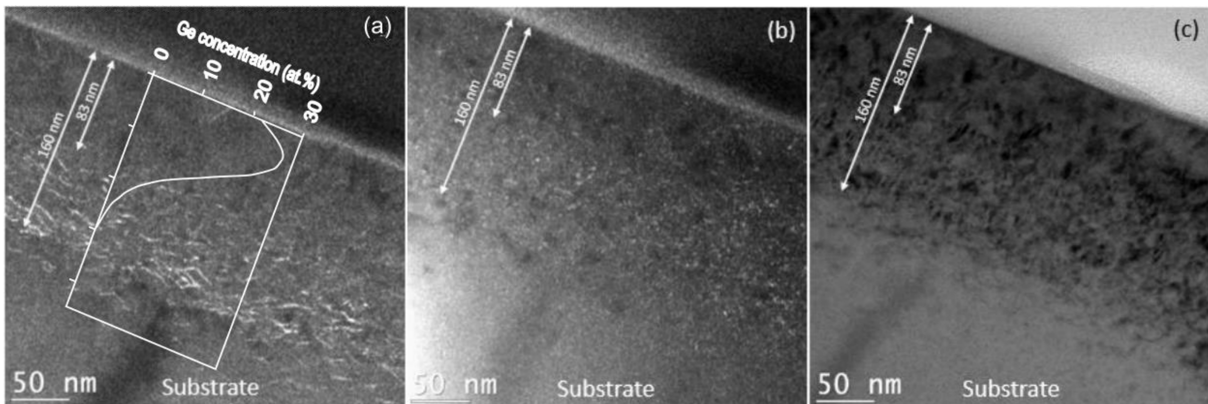


*Figure 9.* TEM images of a sample implanted with $1 \times 10^{17}$ Ge/cm$^2$ at 600 °C and later annealed at 800 °C for 60 minutes under $N_2$ atmosphere. (a) and (b) are in dark-field mode and (c) is in bright-field mode.

## Conclusion

In conclusion, fully relaxed crystalline $Si_{1-x}Ge_x$ films, probably containing dislocations, were formed by Ge implantation in Si, followed by 800 °C annealing. Up to about 30% Ge atoms were incorporated in substitutional sites of the matrix. This concentration saturates for implantations fluences exceeding $1 \times 10^{17}$ Ge/cm², due to sputtering effects becoming important

above 8 × $10^{16}$ Ge/cm². We also showed that the germanium concentrations measured by RBS and XRD are very similar, which means that all Ge atoms could be involved in the formation of the $Si_{1-x}Ge_x$ alloy, confirming the difficulty of forming Ge nanocrystals in silicon. High density of defects were observed for samples implanted at high temperature.

**References**


[1] Barba D., Wang C., Nélis A., Terwagne G., Rosei F., JAP **123** (2018) 161540

[2] Green, M. A., Bremner, S. P. (2017). Nature Materials, 16, 23–34. https://doi.org/10.1038/nmat4676

[3] Beard, M. C., Knustsen, K. P., Yu, P., Song, Q., Luther, J., Ellingson, R., Nozik, A. J. (2007). Nano Lett., 7, 2506–2512. https://doi.org/10.1021/nl071486l

[4] Trinh, M. T., Limpens, R., de Boer, W. D. A. M., Schins, J. M., Siebbeles, L. D. A., Gregorkiewicz, T. (2012). Nature Photonics, 6(5), 316–321. https://doi.org/10.1038/nphoton.2012.36

[5] Nélis A., Barba D., Terwagne G., JAP **128** (2020) 125705

[6] A. Nélis, I. Vickridge, J.-J. Ganem, E. Briand, and G. Terwagne, JAP **130** (2021) 105701

[7] A. Nélis, E. Haye, and G. Terwagne, TSF 746 (2022) 129135

[8] D. Barba, F. Martin, J. Demarche, G. Terwagne, and G.G. Ross, JAP 114 (2013) 074306